

Engineering an all-optical route to ultracold molecules in their vibronic ground state

Christiane P. Koch^{1,*} and Robert Moszyński²

¹*Institut für Theoretische Physik, Freie Universität Berlin, Arnimallee 14, 14195 Berlin, Germany*

²*Department of Chemistry, University of Warsaw, Pasteura 1, 02-093 Warsaw, Poland*

(Dated: November 21, 2018)

We propose an improved photoassociation scheme to produce ultracold molecules in their vibronic ground state for the generic case where non-adiabatic effects facilitating transfer to deeply bound levels are absent. Formation of molecules is achieved by short laser pulses in a Raman-like pump-dump process where an additional near-infrared laser field couples the excited state to an auxiliary state. The coupling due to the additional field effectively changes the shape of the excited state potential and allows for efficient population transfer to low-lying vibrational levels of the electronic ground state. Repetition of many pump-dump sequences together with collisional relaxation allows for accumulation of molecules in $v = 0$.

PACS numbers: 32.80.Qk, 34.30.+h, 33.80.Ps, 42.50.Hz

Introduction Intense interest in ultracold molecular processes is generated by novel applications in ultracold chemistry [1], quantum information processing [2], or high-precision measurements [3]. Ultracold molecules present themselves as ideal candidates also for coherent control: The utilization of constructive and destructive interferences between different quantum pathways in order to steer a process toward the desired target is not hampered by thermal averaging. Photoassociation (PA) provides a natural framework for merging the fields of ultracold molecules and coherent control. It relies in principle only on the presence of optical transitions: Molecules are created by exciting two colliding ultracold atoms to an electronically excited state with laser light [6]. In a few special cases the shape of the excited state potential causes the probability amplitude to pile up at short distance, and molecules in the electronic ground state can be formed by spontaneous or stimulated emission [7]. PA, as well as photostabilization, can be optimized by a suitable design of laser fields [8, 9, 10]. First experiments aimed at PA with short laser pulses [11] had to struggle, however, with difficulties due to the large spectral bandwidth of femtosecond laser systems and the slow timescales of cold collisions. A recent femtosecond pump-probe experiment could provide evidence for coherent formation of molecules [12]. These excited state molecules have huge bond lengths, i.e. the corresponding wavepackets reside at very large internuclear distance. In order to dump them to the electronic ground state, possibly into a single low-lying vibrational level, the molecules need to be brought to short internuclear distance. Here we address the question how such 'R-transfer' can be achieved for generic excited states.

Field-induced resonant coupling We adapt the coherent control concept of applying a strong (near-) infrared laser field in order to modify the excited state dynamics [13]. As shown in Fig. 1a, the field *induces* a coupling between two otherwise isolated excited state potentials. In previous work, both experimental [13] and theoretic

cal [14], the infrared laser field was employed to *suppress* non-adiabatic transitions. Here, the two excited states are dressed by the coupling field, and the diabatic picture is more appropriate: The coupling field mimics resonant spin-orbit coupling, as it is found, e.g., in the 0_u^+ states of heavy alkali dimers [7]. Resonant spin-orbit coupling leads to appreciable binding energies ($E_b > 1 \text{ cm}^{-1}$) of photoassociated molecules in the electronic ground state [7, 15]. Inducing the coupling by an external field offers the advantage that the position of the potentials' crossing can be tuned. This paves the way to ground state levels with much larger binding energies, all the way down to $v = 0$.

Molecule formation We demonstrate that field-induced resonant coupling allows for 'R-transfer' in a generic excited state potential within a two-color pump-dump scheme [8, 16]. As illustrated in Fig. 1a, molecules in the electronic ground state are formed by (i) a pump pulse exciting a wavepacket in the electronically excited state at large internuclear distance, (ii) wavepacket propagation toward shorter distances, where amplitude gets 'trapped' due to the coupling with an auxiliary excited

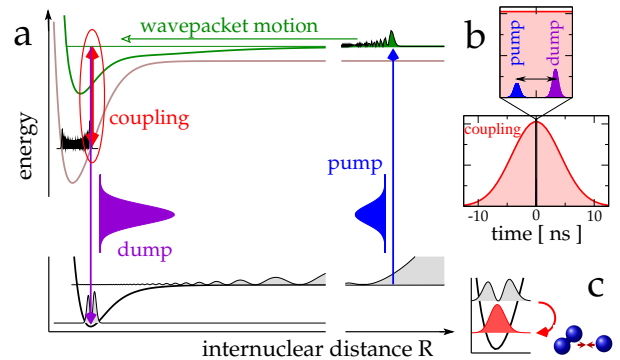


FIG. 1: (color online) Pump-dump photoassociation scheme with a near-IR laser field providing resonant coupling between two excited states: potentials (a), timing of the three fields (b) and collisional relaxation to $v = 0$ (c).

state, and (iii) a dump pulse catching the wavepacket at short distance to transfer it to the electronic ground state. The coupling field amplitude is assumed to be constant during the sequence of pump and dump pulses. Such a constant amplitude can be realized by a nanosecond pulse, given that pump and dump pulses are of a few picoseconds full-width half-maximum (FWHM) and that wavepacket motion takes 50 – 100 ps, cf. Fig. 1b.

Accumulation of ground state molecules The repetition rate of short-pulse laser systems allows for collecting molecules over many identical pump-dump sequences provided that two conditions are fulfilled. (1) The time between two sequences is long enough for the system to equilibrate to the same initial state. (2) Molecules transferred to $v = 1$ by the dump pulse must be removed from $v = 1$ before the next dump pulse arrives in order not to be reexcited. A truly irreversible scheme is obtained if the molecules *decay* to $v = 0$, e.g. due to collisions with atoms. While condition (1) is easily fulfilled for a kHz-repetition rate, the timescale related to condition (2) is given by the inverse of the collisional rate coefficient ($\sim 10^{-10} \text{ cm}^3/\text{s}$ [17]) times the density of atoms, i.e. τ varies between 1 s and 10^{-4} s from MOT to BEC densities.

Model The Hamiltonian describing the situation depicted in Fig. 1a reads

$$\hat{\mathbf{H}}_{\text{gen}} = \begin{pmatrix} \hat{\mathbf{H}}_g & \hat{\boldsymbol{\mu}}_1 \cdot \mathbf{E}(t) & 0 \\ \hat{\boldsymbol{\mu}}_1 \cdot \mathbf{E}^*(t) & \hat{\mathbf{H}}_e & \hat{\boldsymbol{\mu}}_2 \cdot \mathbf{E}(t) \\ 0 & \hat{\boldsymbol{\mu}}_2 \cdot \mathbf{E}^*(t) & \hat{\mathbf{H}}_{aux} \end{pmatrix}, \quad (1)$$

where $\hat{\mathbf{H}}_i = \hat{\mathbf{T}} + V_i(\hat{\mathbf{R}})$ denotes the vibrational Hamiltonian of single channel i ($i = g, e, aux$), $\hat{\boldsymbol{\mu}}_j$ the transition dipole moment, and $\mathbf{E}(t) = E_{0,1}S_1(t)\cos(\omega_1 t) + E_{0,2}S_2(t)\cos(\omega_2 t)$. The pump and dump pulses can be considered separately (with $E_1(t)$ corresponding to either one of them) since wavepacket propagation in the excited state is slow and the time delay between pump and dump pulses correspondingly long. In the rotating-wave approximation (RWA), $E_1(t)$ couples only to $\hat{\boldsymbol{\mu}}_1$, and $E_2(t)$ only to $\hat{\boldsymbol{\mu}}_2$. The Hamiltonian is represented on a grid using an adaptive grid step [18], and the time-dependent Schrödinger equation is solved with the Chebychev propagator.

Application to alkaline earth dimers The $^{40}\text{Ca}_2$ dimer is chosen as our prototype system. The interest in ultracold alkaline-earth and alkaline-earth like systems such as ytterbium had been triggered by the quest for new optical frequency standards. Using continuous-wave lasers, PA was observed for calcium and strontium as well as for ytterbium near both the $^1S_0 - ^1P_1$ atomic resonance [19, 20, 21] and the $^1S_0 - ^3P_1$ intercombination line [22, 23, 24]. However, the formation of molecules in the electronic ground state has not been reported to date.

Choice of electronic states The pump-dump sequence is chosen to utilize a dipole-allowed transition proceeding

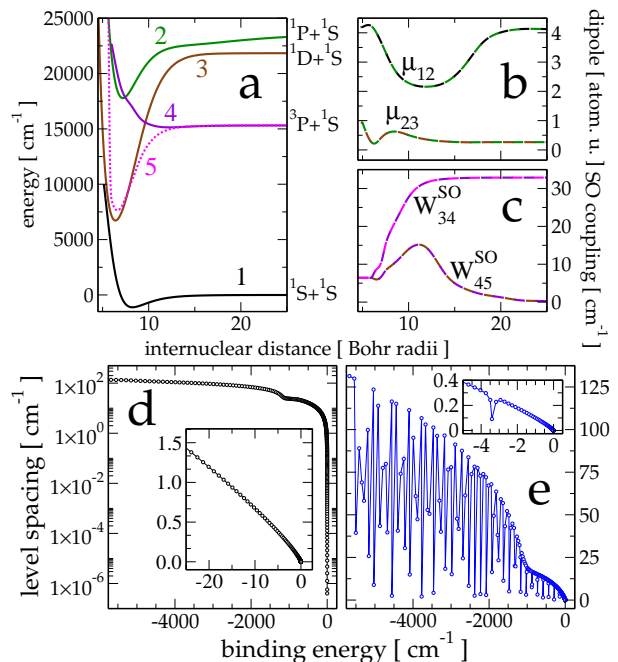


FIG. 2: (color online) Minimal model for Ca_2 including all relevant physics: potential energy curves (a), transition dipole moments (b), and spin-orbit couplings (c) with labels corresponding as $1-X^1\Sigma_g^+$, $2-B^1\Sigma_u^+$, $3-(1)^1\Pi_g$, $4-(1)^3\Sigma_g^+$, $5-(1)^3\Pi_g$. Spacings of the vibrational levels of the $B^1\Sigma_u^+$ excited state (d) and of the $B^1\Sigma_u^+$ and $(1)^1\Pi_g$ states (e) dressed by a moderate near-IR laser field ($I = 3.2 \times 10^9 \text{ W/cm}^2$, $\omega_L = 881 \text{ nm}$). The red box in (d) indicates the range relevant for PA.

via the $B^1\Sigma_u^+$ excited state. The excited state lifetime $\sim 5 \text{ ns}$ does not incur losses in a coherent molecule formation scheme completed in $\sim 100 \text{ ps}$. The $B^1\Sigma_u^+$ state is well suited for PA [19]: Its $1/R^3$ long-range behavior gives rise to large free-bound Franck-Condon factors close to the dissociation limit. However, its vibrational wavefunctions, cf. Fig. 1a, are not favorable to the formation of molecules in their electronic ground state, and spontaneous or stimulated emission will simply redissociate the molecules. Therefore the $B^1\Sigma_u^+$ excited state is coupled to an auxiliary state, chosen to be $(1)^1\Pi_g$. Of all states which have a dipole-allowed transition to the $B^1\Sigma_u^+$ state, $(1)^1\Pi_g$ is closest in energy, with transition frequencies corresponding to infrared (IR) and near-IR lasers. Such small transition frequencies avoid undesirable multi-photon excitations which otherwise may be caused by the coupling field. For $(1)^1\Pi_g$ as auxiliary state in Eq. (1), a three-channel picture is not adequate since the spin-orbit interaction couples it at short range to the $(1)^3\Sigma_g^+$ state which in turn is coupled to the $(1)^3\Pi_g$ state. A minimal model adapting Eq. (1) to Ca_2 comprises of the five channels shown in Fig. 2a. The potential energy curves for calcium are accurately known from spectroscopy [25] as well as from state-of-

the-art *ab initio* calculations [26]. The potentials, transition dipole moment and spin-orbit coupling functions employed in the following calculations are gathered from Ref. [26] and shown in Fig. 2 a-c. In order to estimate how strongly the spin-orbit coupling perturbs the levels of $^1\Pi_g$ state, the five-channel Hamiltonian was diagonalized with $E_{1,2}(t) = 0$. While predissociation of some $^1\Pi_g$ levels is observed above the $^3P + ^1S$ dissociation limit, below that the effect of spin-orbit coupling is negligible. Utilizing only $^1\Pi_g$ levels below the $^3P + ^1S$ dissociation limit corresponds to $\lambda_c < 1200$ nm for the coupling laser. A model comprising of the three singlet channels is then sufficient.

Wavepacket dynamics A sample pump-dump sequence is illustrated by wavepacket snapshots in Fig. 3a with time proceeding from left to right: The initial scattering state (dashed line with light-grey filling in Fig. 3a) describes two atoms colliding in the $X^1\Sigma_g^+$ ground electronic state. A small part of this state is excited by the pump pulse (FWHM=10 ps, $\Delta = -3.5$ cm $^{-1}$, $\mathcal{E} = 0.3$ nJ [33]), forming a wavepacket in the $B^1\Sigma_u^+$ excited state and leaving a hole in the ground state wavefunction (left column of Fig. 3a). Under the influence of the excited state potential, this wavepacket moves toward shorter internuclear distances where the coupling laser ($\lambda_c = 881$ nm, $I = 3.2 \times 10^9$ W/cm 2) cycles population back and forth between the $B^1\Sigma_u^+$ excited state and the $^1\Pi_g$ auxiliary state. The time delay between pump and dump pulses is chosen such that the peak of the dump pulse concurs with a maximum of population in the auxiliary state (center column of Fig. 3a). The dump pulse (FWHM=10 ps, $\Delta = 1016.2$ cm $^{-1}$, $\mathcal{E} = 1.0$ μ J) drives transitions from the excited state to the electronic ground state, populating $v = 1$ (right column of Fig. 3a). This population transfer is due to a *dynamic* interplay of dump pulse and coupling field: As the dump pulse depletes any excited state population within its Franck-Condon window, the coupling field refills it, i.e. population is channelled from the auxiliary through the excited to the electronic ground state. For stronger dump pulses, the depletion of the excited state occurs faster, and refilling this population shows a larger effect. The resulting dependence of the transfer probability on the dump pulse energy is demonstrated in Fig. 3b.

Choice of the laser fields The wavelength of the coupling laser field, λ_c , dictates the internuclear distance R_c at which the excited and auxiliary states cross in a dressed-state picture, cf. Fig. 1a. Since R_c becomes the Franck-Condon point for the dump step, λ_c also determines the target vibrational level in the electronic ground state. To dump into $v = 1$ ($v = 4$), λ_c needs to be 881 nm (1080 nm). The maximum value of λ_c is given by the minimum difference potential of the two states and amounts to roughly 5 μ m (corresponding to a target level bound by ~ 30 cm $^{-1}$). For wavelengths larger than 1200 nm, however, care has to be taken not to couple a predissociated

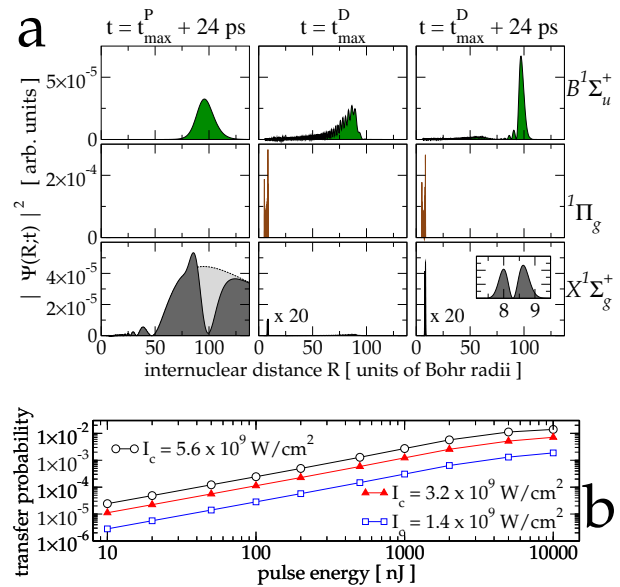


FIG. 3: (color online) Dynamics of the pump-dump photoassociation process under the influence of a moderately strong near-IR laser field ($I = 3.2 \times 10^9$ W/cm 2 , $\lambda_c = 881$ nm): The squared amplitude of the wavefunction in the three states is shown just after the pump pulse ($t = t_{max}^P + 24$ ps), at the maximum of the dump pulse ($t = t_{max}^D = t_{max}^P + t_{delay}$ with $t_{delay} = 83$ ps), and at the end of the whole process ($t = t_{max}^D + 24$ ps). The dashed line with light-grey filling in the lowest left panel corresponds to the initial scattering wavefunction. In the lowest middle and right panel only population which was transferred by the dump pulse to the electronic ground state is plotted. (b) Transfer probability from the excited states to $v = 1$ of the electronic ground state for different intensities of the near-IR coupling laser.

$^1\Pi_g$ -level to the $B^1\Sigma_u^+$ state. Depending on the predissociation width, this could lead to a loss of population. The intensity of the coupling laser field is determined by the requirement that the coupling between the excited and the auxiliary state potentials, $\hat{\mu}_2 \langle E_2(t) \rangle$, be larger than the vibrational level spacing in one of the potentials (cf. Fig. 1 of Ref. [14]). The level spacings of the $B^1\Sigma_u^+$ state are on the order of 1 cm $^{-1}$ for the range of vibrational levels accessed by PA as shown in the inset of Fig. 2d. The requirement on the coupling strength then translates into peak intensities of the order 10^9 W/cm 2 , assuming a typical transition dipole moment of one atomic unit. Such moderate intensities ensure that the coupling laser does not drive multi-photon transitions which could incur losses. Intensities at which multi-photon processes are to be expected can be estimated by comparing calculations without invoking the RWA in Eq. (1) to those performed in the RWA. Increasing the intensity of the coupling laser reveals a breakdown of the RWA at $I \sim 1 \cdot 10^{10}$ W/cm 2 .

For the pump-dump sequence, pulses with transform-limited FWHM of a few picoseconds are best suited with respect to both spectral bandwidth and timescales

[8, 16, 27, 28]. Pulse energies of less than 1 nJ are sufficient in the pump step to excite all population within the resonance window (cf. lower left panel of Fig. 3a). Stronger pulses will not lead to higher PA efficiencies. For the dump step, however, increasing the pulse energy from 10 nJ to 10 μ J yields better population transfer to the target level, cf. Fig. 3b (such pulse energies can be produced by an amplifier). The detuning of the dump pulse is obtained in terms of the binding energies of the target level and of the excited state wavepacket, i.e. the pump detuning. The pump pulse detuning needs to be chosen such that those excited state levels are populated which are indeed perturbed by the coupling laser. The position of the perturbed levels depends rather sensitively on the coupling. Most likely it cannot be theoretically predicted with sufficient accuracy. However, as Fig. 2e indicates, the position of the perturbed levels and hence the pump pulse detuning can be determined experimentally, by performing spectroscopy on the dressed states. In analogy to resonant spin-orbit coupling in alkali dimers [15], the perturbed levels are identified by peaks in the level spacings (or in the rotational constants) as a function of binding energy, cf. Fig. 2e. All other information required for the implementation of the proposed scheme can reliably be obtained from theoretical calculations.

Efficiency An average over all thermally populated initial states [29] yields the number of excited state molecules created by one pump pulse. Assuming the MOT conditions of Ref. [30], $N_{mol} = 12.5$ is obtained. With a dump transfer probability of 10^{-2} , cf. Fig. 3b, and a 10 kHz-repetition rate, one molecule per ms is created in $v = 1$. Collisional decay to $v = 0$ within 1 ms requires a density of 10^{13} cm^{-3} . For lower densities, cavity-enhancement can be used to speed up the decay [31].

Conclusions Resonant coupling in two excited state potentials can be mimicked by applying a near-IR laser field. This paves the way for Raman transitions deep into the well of the electronic ground state. Necessary ingredients for such a pump-dump scheme are (i) an excited state potential with $1/R^3$ long-range behavior and with a dipole allowed transition to the electronic ground state and (ii) an auxiliary state with a dipole allowed transition to the excited state in the (near-)IR. If the equilibrium distance of the auxiliary state is smaller than that of the electronic ground state, the vibronic ground state can be reached in a single pump-dump sequence. The required intensities of the near-IR field are moderate and can easily be produced for nanosecond pulses. Limiting factors are the low PA yield due to the small number of atoms at sufficiently short range, and the slow collisional decay. The PA yield could be improved e.g. by flux enhancement [32], and faster decay can be achieved via cavity-enhancement [31]. Field-induced resonant coupling can be utilized to enhance transition probabilities in any other Raman-like pulsed scheme such as that of Ref. [10] and is therefore expected to be useful well be-

yond photoassociation.

Acknowledgements We are grateful to A. Osterwalder and R. Kosloff for their comments on the manuscript and to the Deutsche Forschungsgemeinschaft (Emmy Noether grant) and the Polish Ministry of Science and Higher Education (grant 1165/ESF/2007/03) for financial support.

-
- * Electronic address: ckoch@physik.fu-berlin.de
- [1] R. V. Krems, *Int. Rev. Phys. Chem.* **24**, 99 (2005).
 - [2] A. Micheli, G. K. Brennen, and P. Zoller, *Nature Phys.* **2**, 341 (2006).
 - [3] T. Zelevinsky, S. Kotochigova, and J. Ye, *Phys. Rev. Lett.* **100**, 043201 (2008).
 - [4] S. A. Rice and M. Zhao, *Optical control of molecular dynamics* (John Wiley & Sons, New York, 2000).
 - [5] P. Brumer and M. Shapiro, *Principles and Applications of the Quantum Control of Molecular Processes* (Wiley Interscience, 2003).
 - [6] K. M. Jones et al., *Rev. Mod. Phys.* **78**, 483 (2006).
 - [7] C. M. Dion et al., *Phys. Rev. Lett.* **86**, 2253 (2001).
 - [8] C. P. Koch, E. Luc-Koenig, and F. Masnou-Seeuws, *Phys. Rev. A* **73**, 033408 (2006).
 - [9] C. P. Koch et al., *Phys. Rev. A* **70**, 013402 (2004).
 - [10] A. Pe'er et al., *Phys. Rev. Lett.* **98**, 113004 (2007).
 - [11] W. Salzmann et al., *Phys. Rev. A* **73**, 023414 (2006). B. L. Brown, A. J. Dicks, and I. A. Walmsley, *Phys. Rev. Lett.* **96**, 173002 (2006).
 - [12] W. Salzmann et al., *Phys. Rev. Lett.* **100**, 233003 (2008).
 - [13] B. J. Sussman et al., *Science* **314**, 278 (2006).
 - [14] J. González-Vázquez et al., *Chem. Phys. Lett.* **431**, 231 (2006).
 - [15] H. K. Pechkis et al., *Phys. Rev. A* **76**, 022504 (2007).
 - [16] C. P. Koch, R. Kosloff, and F. Masnou-Seeuws, *Phys. Rev. A* **73**, 043409 (2006).
 - [17] P. Staunum et al., *Phys. Rev. Lett.* **96**, 023201 (2006). N. Zahzam et al., *Phys. Rev. Lett.* **96**, 023202 (2006).
 - [18] V. Kokoouline et al., *J. Chem. Phys.* **110**, 9865 (1999).
 - [19] G. Zinner et al., *Phys. Rev. Lett.* **85**, 2292 (2000).
 - [20] Y. Takasu et al., *Phys. Rev. Lett.* **93**, 123202 (2004).
 - [21] S. B. Nagel et al., *Phys. Rev. Lett.* **94**, 083004 (2005).
 - [22] R. Ciuryło et al., *Phys. Rev. A* **70**, 062710 (2004).
 - [23] S. Tojo et al., *Phys. Rev. Lett.* **96**, 153201 (2006).
 - [24] T. Zelevinsky et al., *Phys. Rev. Lett.* **96**, 203201 (2006).
 - [25] C. Degenhardt et al., *Phys. Rev. A* **67**, 043408 (2003). O. Allard et al., *Phys. Rev. A* **66**, 042503 (2002). O. Allard et al., *Eur. Phys. J. D* **26**, 155 (2003).
 - [26] B. Bussery-Honvault, J.-M. Launay, and R. Moszynski, *Phys. Rev. A* **68**, 032718 (2003). B. Bussery-Honvault and R. Moszynski, *Mol. Phys.* **104**, 2387 (2006).
 - [27] J. Vala et al., *Phys. Rev. A* **63**, 013412 (2000).
 - [28] E. Luc-Koenig et al., *Phys. Rev. A* **70**, 033414 (2004).
 - [29] C. P. Koch et al., *J. Phys. B* **39**, S1017 (2006).
 - [30] J. Grünert and A. Hemmerich, *Phys. Rev. A* **65**, 041401 (2002).
 - [31] G. Morigi et al., *Phys. Rev. Lett.* **99**, 073001 (2007).
 - [32] S. D. Gensemer and P. L. Gould, *Phys. Rev. Lett.* **80**, 936 (1998).
 - [33] Detunings Δ are taken with respect to the $^1P + ^1S$ dissociation limit, pulse energies \mathcal{E} are calculated assuming a beam radius of 100 μm .